

Synthesis, Characterization and Sustainability by Utilisation of Psidium Guajava-Iron Nano particles (PG-FeNPs) for the removal of Methylene blue Dye

Kaza Kusuma Jayasree Komali¹, Lingam Anjali¹, Balam Krishna Sri Pragnya², Satti Amrutha^{2*}, and Meena V⁵

¹B. Tech Biotechnology, Department of Chemical Engineering, Andhra University College of Engineering, Visakhapatnam, Andhra Pradesh, India.

²B. Tech Chemical Engineering, Department of Chemical Engineering, Andhra University College of Engineering, Visakhapatnam, Andhra Pradesh, India.

Abstract. Water is the only liquid that sustains all life and acts as catalyst to initiate their metabolisms. It is more essential to life than all other nutrients put together. Life becomes impossible without water. In the past few years, one of the most important environmental crisis has been the contamination of water resources. Using Psidium guajava leaves as adsorbents, the current work aims to extract methylene blue from an aqueous solution. The variables that were examined include temperature, average particle size of adsorbents, initial dye concentration, contact time, solution pH, adsorbent dosage. The adsorption of methylene blue onto Psidium guajava leaves as adsorbents was studied using a variety of isotherm models, including Langmuir, Freundlich, Temkin, and Redlich-Peterson (R-P) as well as kinetic studies of Pseudo (first & second) order [23]. Thermodynamic parameters were also estimated for the extraction of Methylene blue onto both the adsorbents. The analysis of adsorbents was depicted by using Field Emission Scanning Electron Microscopy (FE-SEM) and Fourier Transform Infrared Spectroscopy (FTIR) for their surface morphology and surface functional groups, respectively [20].

1 Introduction

Nanotechnology can be achieved through two main approaches: bottom-up and top-down. In the bottom-up approach, individual atoms and molecules are meticulously arranged to form nanoparticles with specific sizes and shapes. This is achieved by controlling deposition or reduction processes. Top-down approaches, conversely, involve sculpting nanoparticles from bulk materials by extracting unwanted atoms and molecules.

* Corresponding Author: 320106205008@andhrauniversity.edu.in

Nanoparticles are synthesized using physical and chemical methods. However, these methods often raise concerns due to their potential toxicity and negative impact on the environment and living organisms. Psidium guajava leaves can be used to create iron nanoparticles. These nanoparticles function as both reducing and capping agents. Iron nanoparticles smaller than a micro meter, known as nanoscale iron particles, have various applications. They are being explored for environmental remediation purposes, particularly in cleaning up industrial sites contaminated with chlorinated organic compounds.

1.1 Toxicity of Some Contaminants

Industries generate waste water with enormous number of concentration of pollutants. The consequences of toxic dyes incorporate dermatitis, mild allergies, gastric ulcers, asthma and even cancer. Some azo dyes can cause cancer. Additionally, the breakdown of the azo group in certain dyes can make them mutagenic.

1.2 Toxicity of Some Synthetic Dyes

Dyes are widely utilised in the textile industry to color fabrics like nylon, wool, silk, and cotton. However, these dyes pose a threat to the environment when dye-laden effluents are released into waterways after industrial processes. Beyond the visible water pollution, these dyes disrupt a critical ecological process: photosynthesis in rivers

Synthetic dyes are mainly sourced from petrochemicals and used for hefty scale dyeing operations. A dye molecule normally contains two major components; chromophores and auxochromes [1], [2]. Chromophores are responsible for color upon adsorption of ultraviolet-visible electromagnetic radiation while auxochromes enable the dye to bind onto fibres [3].

According to their structure, it is obvious to categorize dyes as cationic or anionic. These dyes have a net negative charge in liquid media because they include sulfate groups, where as cationic dyes have a net positive charge because they contain sulfur-containing groups or protonated amines.

1.2.1 Anionic dyes

The differentiate aspect of anionic or acid dye is their water solubility and ionic substituents [4]. They depend on a negative ion and include a wide range of dyes such as anionic azo along with reactive dyes [6]. The nearness of sweet-smelling and sulphonic bunches makes acid dyes hurtful to people and different microorganisms.

1.2.2 Cationic dyes

Dyes that are basic or cationic dissolve easily in water to produce colored cations. Due to the substituted aromatic groups in their structure, these dyes are poisonous and can cause skin irritation, allergies, and mutations [5]. Methylene blue is a cationic dye sample

2 Raw materials and removal processes:

2.1 Synthesis of Psidium guajava leaves extract

Here Psidium guajava leaves were collected. FeCl₃ solutions were mixed with the appropriate leaf extract to generate iron nanoparticles. Ten grams of leaves were used to create individual leaf extracts [7]. Ten grams of leaf extract are added to a 100 ml volume of deionized water in a conical flask. The mixture needs to heat at 80°C for ten minutes. Put the mixture through what's guy filter paper once it has warmed up to room temperature. After up to a week of storage at 4oC, this filtrate can be used.



Fig-1. Leaves of Psidium guajava

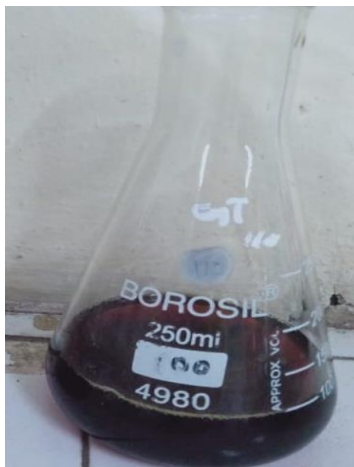


Fig-2. Extract of Psidium guajava

2.2 Iron nanoparticles synthesis:

Ferric chloride was added to the extract of Psidium guajava leaves to produce iron nanoparticles. Mix 8.11 grams of Ferric chloride granulate in 500 milliliters of water. A

mixture of 1:1 volume ratio of the above Ferric chloride solution and Psidium guajava leaves after filtration is made. Using a mechanical stirrer, the mixture should be stirred when it is at room temperature. The quick formation of a black precipitate indicates that the Fe²⁺ ion concentration is going to drop. The precipitates were then centrifuged for 20 minutes at 5000 rpm. Ultimately, the iron nanoparticles were sent into a vacuum oven and dried continuously for three hours at 65⁰ c.



Fig-3. PG-Fe.is synthesized



Fig-4. PG-FeNP. Is centrifuged



Fig -5. FeNP. Is dried

2.3 Scanning Electron Microscope (SEM) Images:

The minute structures and range of sizes of PG-FeNP are clearly visible in the Scanning Electron Microscop pictures in Figures 6 and 7. It shows that the probe currents are stable and have great resolution for the best possible imaging. The size range of the produced nanoparticles was 159.3–250.6 nanometers[27].

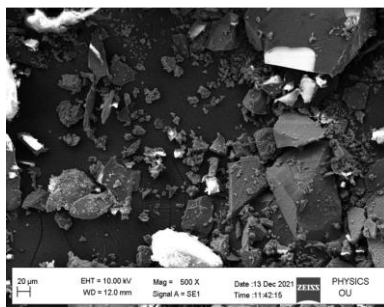


Fig -6 ahead of synthesis.

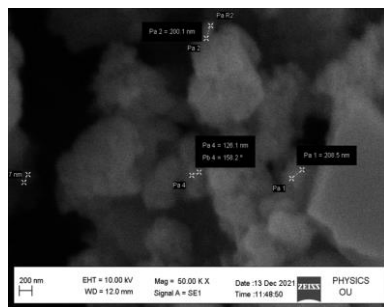


Fig -7. posterior of synthesis.

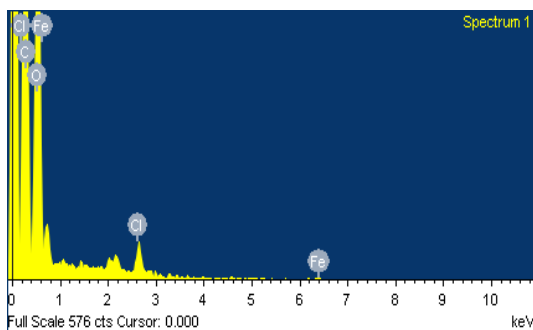


Fig -8. Graphical representation

2.4 Diffraction of X-Ray (XRD):

Peak locations in the figure point to the development of a hexagonal wurtzite crystal structure. At two values, the PG-FeNPs maxima are 10.920, 5.740, 17.940, 22.310, 28.520, and 30.520. Ninth figure displays PG-NPs X-Ray Diffraction.

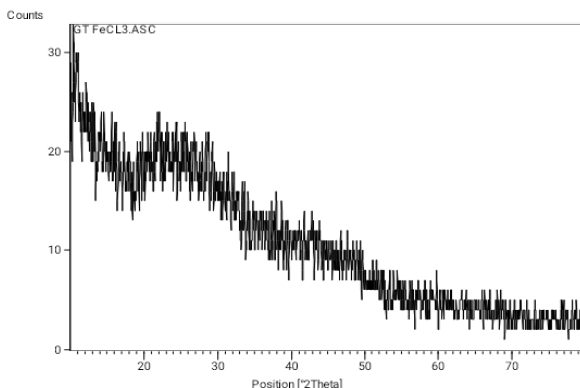


Fig -9. X-Ray Diffraction pattern

2.5 Fourier Transform Infrared Spectroscopy (FTIR):

Peak locations in the figure point to the development of a hexagonal wurtzite crystal structure. At two values, the PG-FeNPs maxima are 10.920, 5.740, 17.940, 22.310, 28.520, and 30.520. Figure 9 displays the PG-NPs XRD.

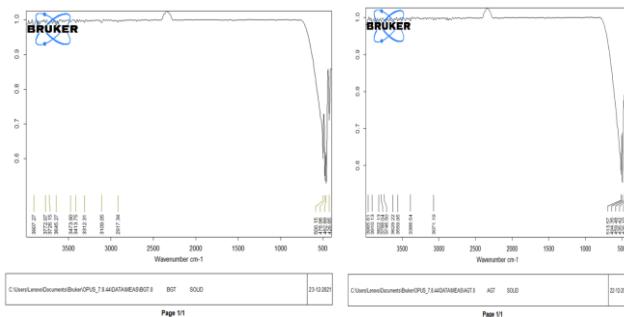


Fig-10. analysis of PG-FeNPs before and after FTIR

3 Results and Discussions

Plots and a thorough description using multiple isotherms are used to display the data from the numerous tests that were undertaken. Studies on kinetics and thermodynamics were also given. Many experimental runs were carried out in an attempt to investigate the effects of different process factors on the percentage of dye removal and dye uptake, including contact time, solution pH, beginning dye concentrations, adsorbents dose, average particle size of the adsorbents, and temperature.

3.1 Adsorption of Methylene blue onto Psidium guajava

Adsorption is the process by which biological material removes or binds a desired component from an aqueous solution. These materials can exist in soluble or insoluble forms, and they can be both organic and inorganic. As a result, Psidium guajava adsorbents

were chosen to separate Methylene blue from an aqueous solution. With the use of plots related to the numerous experimental experiments carried out, the following subsections present the findings and pertinent considerations.

3.1.1 Contact time:effect

An important factor is the contact time, or the amount of time dye molecules are in the aqueous solution and to get in touch along the adsorbent that is being utilized to remove the dye.

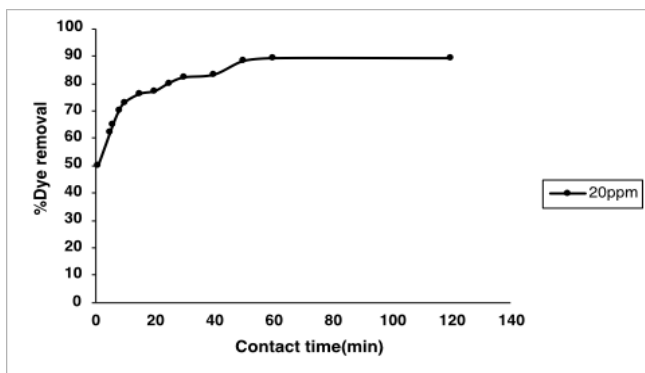


Fig 11: Plots show the effect of contact time on % dye removal of Methylene blue using Psidium guajava ($C_i = 20-100$ mg/L, $m = 0.1$ g, $d_p = 75$ μ m, $V = 30$ ml, $RPM = 180$, $T = 303$ K).

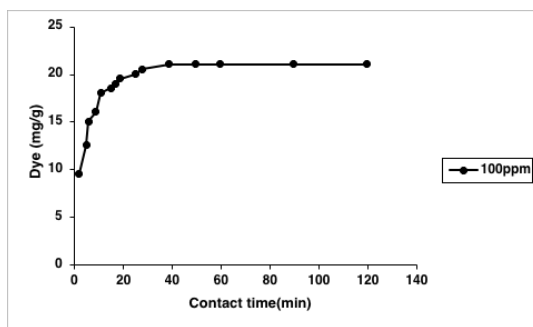


Fig 12: Plots show how Psidium guajava adsorbents dye uptake is effected by contact time. ($C_i = 20-100$ mg/ml, $m = 0.1$ g, $d_p = 75$ μ m, $v = 30$ ml, $RPM = 180$, $T = 303$ K). plot in fig 5.1.2 shows that Psidium guajava dye uptake increased from 2.970 to 5.325mg/g at an initial dye concentration of 20mg/L with an increase in contact duration from 2 to 60 min. similar patterns were also noted when the original dye concentration were varied.. additionally, for Psidium guajava the consumption of the dye hiked from 10.203 to 2.723 at higher initial dye concentrations with an increase in contact time from 2 to 60 min

3.1.2 solution pH Effect

Effect of pH effect of pH on percentage dye removal and dye uptake of Psidium guajava leaves adsorbents was studied separately at constant temperature and speed of agitation of 303 K & amp; RPM = 180, along various values of initial dye concentrations (20 up to 100

milligrams per litre), from 2 to 10 in the pH of the solution. The experimental results of the pH's influence on the percentage of dye removed and the dye uptake of methylene blue for both adsorbents are displayed in fig 5.1.3 and 5.1.4. it is clear that pH plays a significant role in dye clearance.

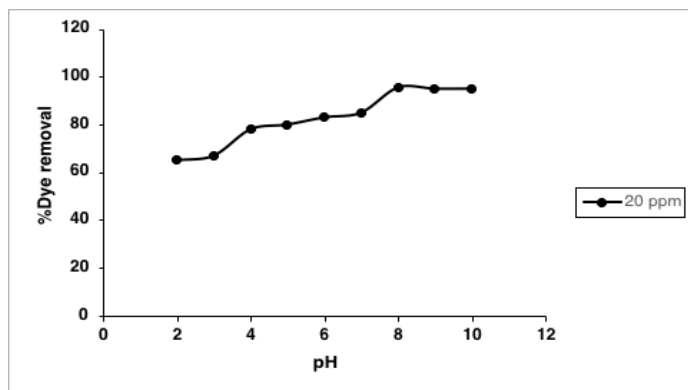


Fig 13: Plots (a), (b) show the response of solution pH on % dye removal of Methylene blue using Psidium guajava adsorbents ($C_i = 20-100\text{mg/L}$, $m=0.1\text{ g}$, $d_p = 75\ \mu\text{m}$, $V=30\text{ ml}$, $\text{RPM}=180$, $T=303\text{ K}$, $t=60\text{ min}$).

From the plots (b) in Fig 13 for an initial dye concentration of 20 milligrams per litre, it was studied that if we increase the solution pH from 2 to 8, an increment in % dye removal is seen from 64.70 to 92.94% for Psidium guajava adsorbents. Psidium guajava adsorbents with an increase in pH from 2 to 8.

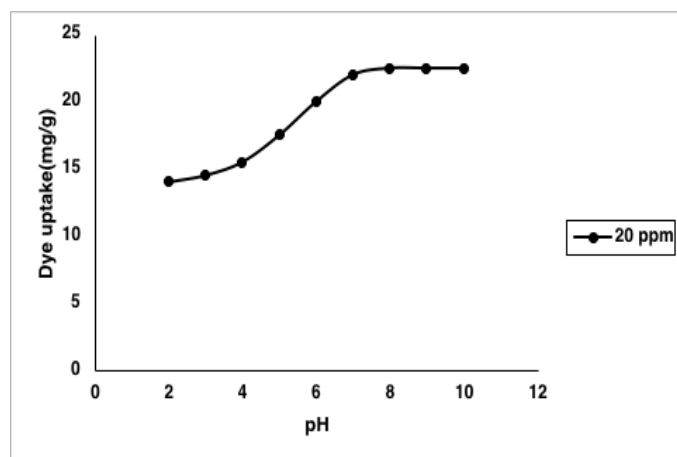


Fig 14: Plots (b) show the solution effect on pH dye uptake in Psidium guajava adsorbents ($C_i = 20 - 100\text{ mg/L}$, $m=0.1\text{ g}$, $d_p = 75\ \mu\text{m}$, $V=30\text{ml}$, $\text{RPM}=180$, $T=303\text{ K}$, $t=60\text{ min}$).

Similar to Fig 14, the plots in Fig 5.1.4 show an increasing dye uptake with an rise in pH from 2 to 8 and the dye uptake is insensitive to further increase in pH value. Further, it is also observed that, at any particular value of pH, the dye uptake is considerably less for low initial dye concentrations when compared to dye uptake values at high initial dye concentrations.

3.1.3. Temperature effect

The temperature of solution also has some influence on the % dye removal from aqueous solution. In general higher solution temperatures may propel the diffusion rate over the peripheral layer and also may enhance the interior pore of the adsorbent.

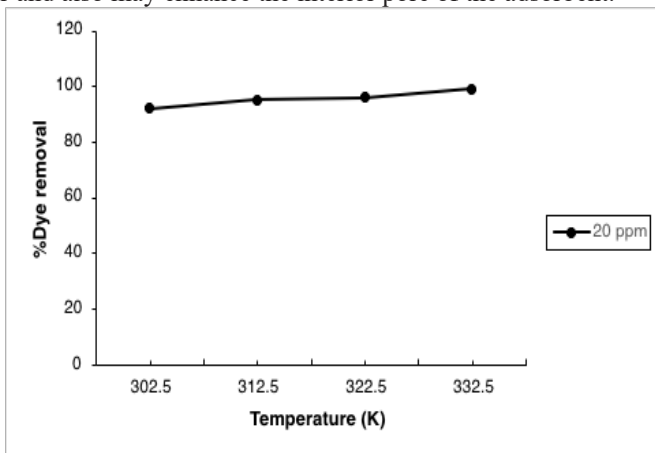


Fig 15: Plots (a), (b) show the consequence of change in temperature on % dye removal of Methylene blue onto, Psidium guajava adsorbents ($C_i = 2-100$ mg/L, $m=0.1$ g, $d_p = 75$ μ m, $V=30$ ml, RPM=180, $t=60$ min, pH=8).

The influence of temperature change on the % dye removal of Methylene blue onto Psidium guajava was explored at 303, 313, 323, 333 K and the results are plotted in Figs 15 and 16.

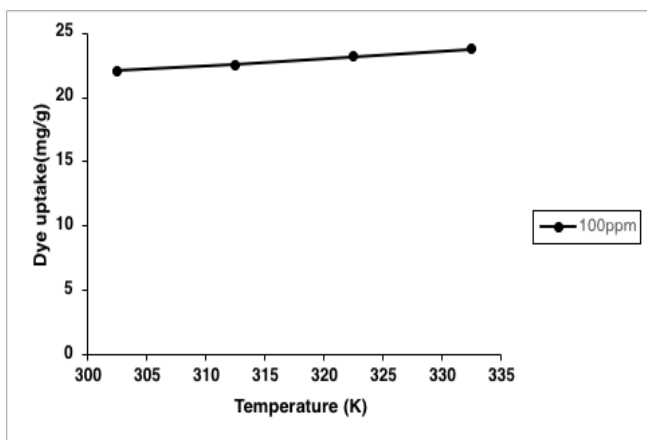


Fig 16: (b) show the consequence of change in temperature on % dye removal of Methylene blue onto Psidium guajava adsorbents ($C_i = 20-100$ mg/L, $m=0.1$ g, $d_p = 75$ μ m, $V=30$ ml, RPM=180, $t=60$ min, pH=8)

3.1.4. Initial dye concentration

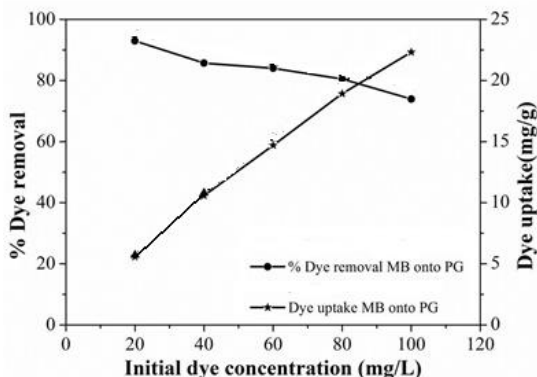


Figure 17: initial dye concentration on percentage of dye removal and dye uptake of Methylene blue using *Psidium guajava* ($T=303\text{ K}$, $m=0.1\text{ g}$, $d_p=75\text{ }\mu\text{m}$, $V=30\text{ ml}$, $\text{RPM}=180$, $t=60\text{ min}$, $\text{pH}=8$). It is evident from these two plots that, 92.94 to 74.42% for *Psidium guajava* adsorbents. These findings show that when the original dye concentration is raised, the percentage of methylene blue dye clearance reduced. Additionally, figure 17 demonstrates that when the initial dye concentration was changed from 20 to 100 mg/L, *Psidium guajava* dye uptake increased from 5.0576 to 22.326 mg/g

3.1.5 Effect of adsorbents dosage

This parameter governs the capacity of an adsorbent for a specific starting adsorbent concentration, when the initial concentration is 20 mg/L, the solution pH is 8, the temperature is maintained constant at 303K, the adsorbents are evaluated for their effects on the percentage dye removal and dye uptake in this section agitation speed of $\text{RPM} = 180$.

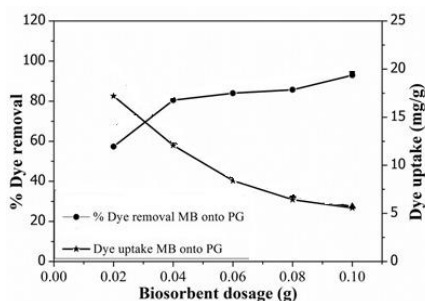


Figure 18: Effect of adsorbents dosage on % dye removal and uptake of Methylene blue using *Psidium guajava* adsorbents ($T=303\text{ K}$, $m=0.1\text{ g}$, $d_p=75\text{ }\mu\text{m}$, $V=30\text{ ml}$, $\text{RPM}=180$, $t=60\text{ min}$, $\text{pH}=8$, $C_i=20\text{ mg/L}$).

The % dye removal escalates extremely with increasing adsorbents dosage up to 0.1 g

3.1.6 Effect of average particle size of adsorbents

The average particle size of the adsorbents is also an important factor which alters the adsorption rate. These plots indicate that both the % dye removal and dye uptake values decreased when the adsorbents average particle size increases. The capacity of smaller

particles to penetrate through the interior pores of adsorbents is particularly great because they have shorter diffusion routes and a higher surface area per unit mass. From Fig 5.1. it can be noticed that, the % dye removal decreased drastically from 92.94 to 60.05 % for *Psidium guajava* adsorbents when the average size of adsorbents is increased from 75 to 300 μm .

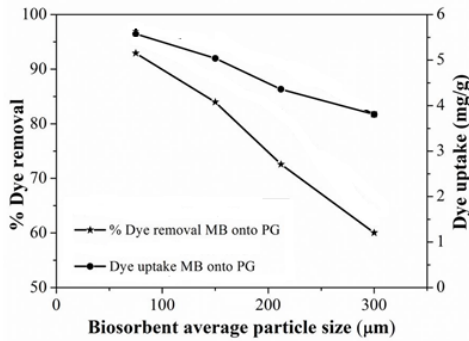


Figure 19: Effect of average particle size on %dye removal and dye uptake of Methylene blue onto *Psidium guajava* adsorbents (T=303 K, m=0.1 g, V=30 ml, RPM=180, t=60 min, pH=8, $C_i=20$ mg/L).

3.2 Equilibrium studies

Data from equilibrium tell us about the adsorbent's capability. These equilibrium investigations are typically presented as isotherms. The phenomenon that controls the retention of a material from aquatic environments on a solid phase at a fixed temperature and pH of the solution is described by any adsorption isotherm.

3.2.1 The Langmuir isotherm for adsorption

The quantitative definition is the Langmuir adsorption isotherm provides a function of the concentration of the adsorbent material in the liquid phase with which it comes into contact and the creation of a molecules layer above the surface of the adsorbent. The following are the presumptions made by the Langmuir theory: Within the biosorbent, specific homogenous sites are where the bio sorption occurs [8]. A dye molecule's occupation of a site prevents further adsorption from occurring there [9].

$$q_{eq} = \frac{b q_{max} C_{eq}}{1 + b C_{eq}}$$

The Langmuir model in linear form is given as

$$\frac{C_{eq}}{q_{eq}} = \frac{1}{b q_{max}} + \frac{1}{q_{max}} C_{eq}$$

The linear plot of C_{eq}/q_{eq} vs C_{eq} 's slope of intercept yields the Langmuir constants q_{max} and bare. Figure 20 displays the Langmuir plots of (C_{eq}/q_{eq} versus C_{eq}) for the 303K

temperature at which Methylene blue is adsorbed onto *Psidium guajava*. According to the slope and intercept, Corresponding *Psidium guajava*'s maximum adsorption capacity (q_{max}) and b values that are calculated are 27.778 milligrams per gram and 0.135 l Litres per milligram.

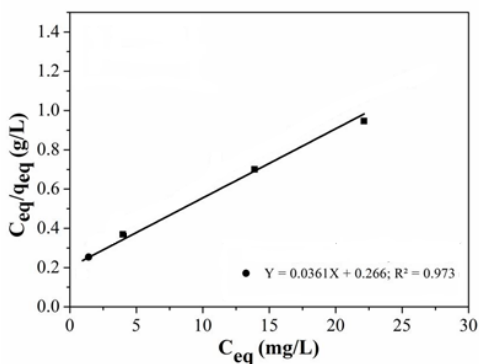


Fig 21: The Langmuir isotherm for the adsorption of Methylene blue onto *Psidium guajava* adsorbents (pH = 8, C_i = 20-100 mg/L, t = 60 min, m = 0.1g, d_p = 75 μ m, V = 30 ml, RPM = 180).

The following equation was used to identify the essential terms for the Langmuir isotherm, which can be represented in terms of the separation factor, or R_L :

$$R_L = \frac{1}{1 + bC_i}$$

The R_L value can be characterized in terms of four probabilities: (i) advantageous adsorption, where the value falls between 0 and 1; (ii) unfavorable adsorption, where the $R_L > 1$; (iii) linear adsorption, where the $R_L = 1$; and (iv) irreversible adsorption, where the $R_L = 0$. For both adsorbents, the R_L values at various concentrations are displayed in Fig. 5.1.11.

Figure 11 illustrates the values of R_L for the adsorption of Methylene blue onto *Psidium guajava* which were found to be in the range of 0.269 to 0.069 respectively.. Given that the R_L value falls between 0 and 1, these results show that Methylene blue was adsorbed favorably onto both adsorbents. Additionally, the R_L values show that adsorption is stronger at lower Methylene blue concentrations.

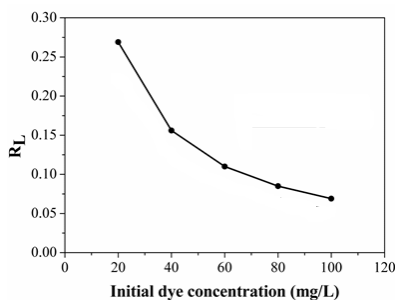


Fig. 22: R_L (Separation Factor) values for adsorption of Methylene blue onto *Psidium guajava* adsorbents.

3.2.2 Freundlich isotherm

This isotherm is employed to fit experimental data collected across a broad range of concentrations. The model for the Freundlich isotherm is provided as [10].

$$q_{eq} = K_F C_{eq}^m$$

Where,

- q_{eq} – Amount of dye absorbed per unit mass of adsorbent at equilibrium (mg/g),
- C_{eq} – Equilibrium concentration (mg/L),
- K_F – Freundlich adsorption constant and

m is a dimensionless constant ($1/n$). Adsorption is homogeneous for $n=1 < 1$ and > 1 , indicating that the adsorption is favorable or unfavorable, accordingly. [4] The Freundlich isotherm can be expressed linearly as $\text{Log } q_{eq} = \text{log } K_F + m \text{ log } C_{eq}$.

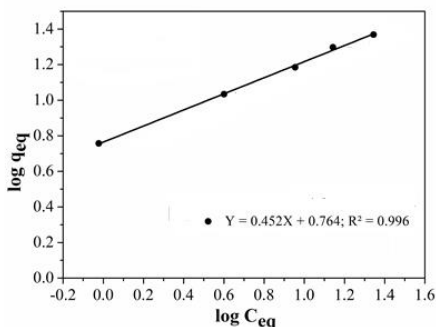


Fig 23: Freundlich isotherm for adsorption of Methylene blue onto *Psidium Guajava* adsorbents (T=303K, m=0.1 g, d_p=75µm, V=30 ml, RPM=180, t=60 min, pH=8, C_i=20-100 mg/L).

3.2.3 Tempkin isotherm

The adsorbent's capacity for adsorbate ion adsorption is assessed using the Tempkin model. According to this concept, interactions between the adsorbant and adsorbate cause the heat of adsorption of every molecule in the layer to decrease linearly with coverage. A uniform distribution of binding energies up to maximal binding energy characterizes adsorption [11]. The expression for the Tempkin isotherm

$$q_{eq} = \frac{RT}{b_T} \ln(A_T C_{eq})$$

$$q_{eq} = \frac{RT}{b_T} \ln C_{eq} + \frac{RT}{b_T} \ln A_T$$

The linear plot of q_{eq} vs C_{eq} for Methylene blue onto the two adsorbents under consideration is depicted in Fig. 24, and Table 5.1.1 provides the parameter values. For *Psidium guajava* adsorbents, the correlation coefficient (R^2) values were found to be strong, at 0.953. These high R^2 values imply that a heterogeneous surface may be the cause of the adsorption process.

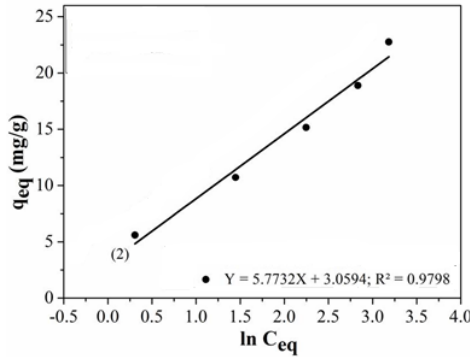


Fig 24: Tempkin isotherm for adsorption of Methylene blue onto *Psidium guajava* adsorbents (T=303 K, m=0.1 g, d_p=75 μm, V=30 ml, RPM=180, t=60 min, pH=8, C_i=20-100 mg/L).

3.2.4 Redlich-Peterson isotherm

Redlich and Peterson isotherm, which can be defined as follows, was proposed by Jossens et al. [13] in order to combine the benefits of both the Langmuir and Freundlich isotherms.

$$q_e = \frac{AC_e}{1 + BC_e^g} \quad (5.1.8)$$

Taking natural logarithm of both sides,

$$\ln\left(\frac{C_{eq}}{q_{eq}} - 1\right) = g \ln(C_{eq}) + \ln(B) \quad (5.1.9)$$

G and B are computed using the values of the slope and the intercept. For *Psidium guajava*, the correlation coefficient (R²) values were determined to be 0.149. These low correlation coefficients indicate that the data do not accord well with this isotherm.

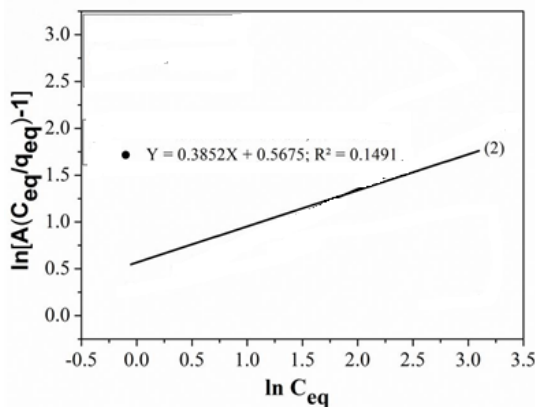


Fig. 25: Redlich-Peterson isotherm for adsorption of Methylene blue onto *Psidium guajava* adsorbents (T=303 K, m=0.1 g, d_p=75 μm, V=30 ml, RPM=180, t=60 min, pH=8, C_i=20-100 mg/L).

Table 1 : Adsorption Isotherm Constants for Removal of Methylene blue onto *Psidium guajava*.

NAME OF THE ISOTHERM	CONSTANTS	PSIDIUM GUAJAVA
Langmuir	b(L/mg)	0.135
	q _{max} (mg/g)	27.778
	R ²	0.996
Freundlich	K _F ((mg/g)(L/mg) ^(1/n))	4.830
	1/n or m	0.476
	R ²	0.996
Tempkin	A _T (L/g)	1.50
	b _t (J/mol)	444.6
	R ²	0.953
Redlich Peterson	g	0.385
	B(L/mg)	1.762
	R ²	0.149

3.3 Kinetic studies

Understanding the sorption mechanism through kinetic studies is essential for optimization process efficiency. These The two most popular pseudo-second order kinetic models are (i) Ho's and (ii) Lagergren's pseudo-first order models. In order to determine the precise process underlying the adsorption of Methylene blue dye, *Psidium guajava* was used as an adsorbent.

3.3.1 Pseudo-first order model

The Pseudo-first order model [14] is the most appropriate kinetic model for low solute concentrations. Its equation is as follows:

$$\frac{dq}{dt} = K_1(q_{eq} - q)$$

Integrating Eq. (5.1.10) with respect to conditions q = 0 at t = 0 to q = q at t = t, the kinetic rate expression becomes:

$$\frac{dq}{dt} = K_1(q_{eq} - q)$$

$$\log(q_{eq} - q) = \log q_{eq} - \frac{K_1}{2.303}t$$

Plots of Log(q_{eq}-q)vs t are used to calculate the pseudo-first order rate constants K₁ & q_{eq} , by examining their slope and intercept. The pseudo-first order kinetic model's linear plots are displayed in Fig.27 plots (a) and (b). The plot of Log(q_{eq}-q) vs t at various starting concentrations(20 to 100 mg/L) of the Methylene blue was used to independently assess the

validity of the pseudo-first order kinetic model for the adsorption of Methylene blue dye using *Psidium guajava* adsorbents. The intercept and slope were used to calculate the values of the equilibrium adsorption capacity and the first order rate constant. these values were then tabulated together with the correlation co efficient values for both adsorbents in the table.

Table 2: Pseudo-First Order Kinetic Model Parameters for Methylene blue Removal using *Psidium guajava* Adsorbents.

Initial dye Conc. (mg/L)	q _{eq, exp} (mg/g)	q _{eq, cal} (mg/g)	K _I (g/ mg.min)	R ²
	PG	PG	PG	PG
20	5.576	2.322	0.048	0.980
40	10.587	5.3088	0.066	0.968
60	14.706	6.137	0.062	0.975
80	18.933	8.550	0.067	0.984
100	22.326	10.0925	0.0598	0.951

3.3.2 Pseudo-second order model

The ratio of solute adsorbed on the adsorbent surface to solute adsorbed at equilibrium determines the pseudo-second order reaction rate in major part[15]. The pseudo-second order equation has the following form:

$$\frac{dq}{dt} = K_{II}(q_{eq} - q)^2$$

Where,

q - dye adsorbed at time t (mg/g)

q_{eq}- The adsorption at equilibrium (mg/g)

K_{II}- The equilibrium rate constant (g/ mg-min) and

t - Time (min).

Applying the initial conditions q = 0 at t = 0 to q = q at t = t and then integrating the above equation results in

$$\frac{t}{q} = \frac{1}{K_{II}q_{eq}^2} + \frac{1}{q_{eq}}t$$

Plots of t/q vs. t were used to assess the validity of the pseudo-second order kinetic model for the adsorption of Methylene blue dye onto *Psidium guajava*. The findings show that the R2 values are getting closer to unity and that the experimental and computed q_{eq} values are quite similar to one another.

Table 3: Pseudo-Second Order Kinetic Model Parameters for Methylene Blue Removal using *Psidium guajava* Adsorbents.

Initial dye Conc. (mg/L)	$q_{eq, exp}$ (mg/g)		$q_{eq, cal}$ (mg/g)		K_{II} (g/mg.min)		R^2	
		PG		PG		PG		PG
20		5.576		5.780		0.030		0.999
40		10.587		11.11		0.015		0.999
60		14.706		16.129		0.009		0.999
80		18.933		21.277		0.006		0.998
100		22.32		25.00		0.005		0.998

3.4 Thermodynamic studies

Studies on thermodynamics are very helpful in determining the nature and viability of the process. We used the computered thermodynamic parameters to determine the affinity, spontaneity, and heat change of the adsorption process: change in free energy, change in enthalpy, and change in entropy. The relationship between the standard free energy change and equilibrium constant is proved by the equation

$$\Delta G^0 = -RT \ln K_a$$

The value of K_a the equilibrium constant is calculated using the following equation,

$$K_a = q_{eq} / C_{eq}$$

where C_{eq} is the equilibrium adsorbate concentration in solution and q_{eq} is the dye absorption.

The adsorption's entropy change (ΔS^0) and enthalpy change (ΔH^0) were calculated using the equation that follows.

$$\begin{aligned} \log(K_a) &= \Delta S^0 / (2.303 R) - \Delta H^0 / (2.303 RT) \\ \Delta G^0 &= \Delta H^0 - T \Delta S^0 \end{aligned}$$

the values of ΔH^0 and ΔS^0 were calculated using the linear adsorbents Van Hoff plot's slope and intercept or $\log(q_{eq}/C_{eq})$ vs. $(1/T)$, if the Gibbs free energy values are between -20 and 0 kJ/mol; chemi-sorption is the term used if the valued are between -400 and -80 kJ/mol.

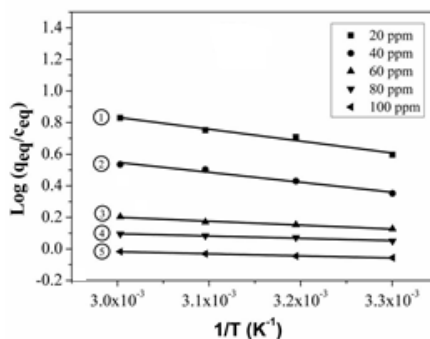


Fig 29: plot illustrating the Van't Hoff relation used to calculate the thermodynamic parameters of methylene blue adsorption onto *Psidium guajava* adsorbents.

The slope and intercept of the linear Van't Hoff plot of $\text{Log} (q_{eq}/C_{eq})$ vs $1/T$ were used to get the values of change in enthalpy and change in entropy, respectively. Tables 5.1.4 and 5.1.5 provide a summary of the findings.

Tables provide the obtained thermodynamic parameters. Indicative of an endothermic process is positive ΔH . Similarly, a positive value of ΔS during the adsorption phase an increase in randomness at the solid state/liquid interface [18]. Enthalpy changes in the 20–40 kJ/mol and 80–400 kJ/mol ranges, respectively, are indicative of physisorption and chemisorption [19]. The ΔH values found in this investigation fall between the 2.552–14.393 kJ/mol and 1.892–22.308 kJ/mol ranges of the physisorption mechanism.

Using oil palm empty fruit fibers[20], chemically altered *Ficus carica*[21], cotton stalk, cotton waste, and cotton dust similar trends were seen for methylene blue.

Table 5: Thermodynamic Parameters for Methylene blue onto *Psidium guajava* Adsorbent

Initial concentration (mg/L)	ΔH (kJ/mol)	ΔS (J/mol K)	ΔG (kJ/mol)			
			303 K	313 K	323 K	333 K
20	14.393	59.126	-3.522	-4.114	-4.705	-5.296
40	12.065	46.681	-2.080	-2.546	-3.013	-3.480
60	4.768	18.132	-0.726	-0.907	-1.089	-1.270
80	2.822	10.301	-0.299	-0.402	-0.505	-0.608
100	2.552	16.371	-2.408	-2.571	-2.735	-2.899

3.5 Characterization of *Psidium guajava* Adsorbents using FE-SEM and FTIR Analyses

The FE-SEM micrograph of *Psidium guajava* adsorbents, respectively, prior to adsorption is shown in Images 30 of Figure 5.1.18. These photos clearly show how extremely diverse the adsorbent is, how rough its surface morphology is, and how likely it is that the dye will be absorbed.

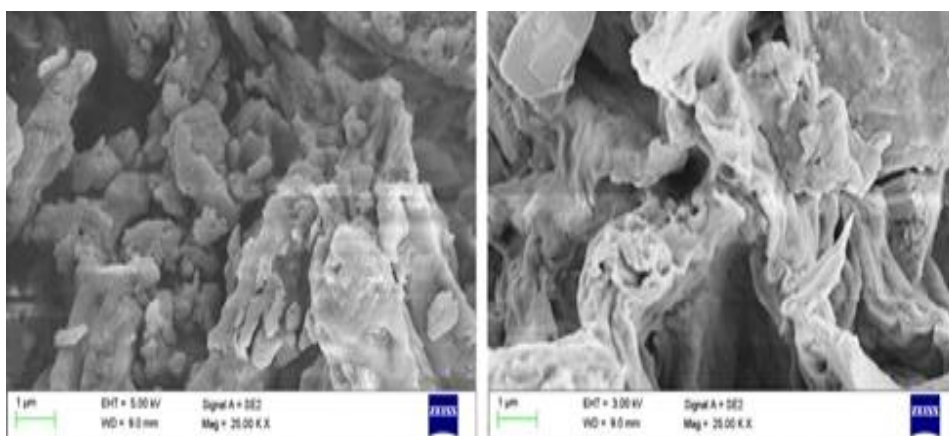


Fig. 30 & 31 : Images 30 and 31 show the FE-SEM micrographs of *Psidium guajava* adsorbents before and after adsorption of Methylene blue onto its surface.

The dye molecules cover the whole surface of the adsorbent dosage, as can be seen from the surface of the dye-loaded adsorbent. Following the adsorption of Methylene, the pores were fully packed with dye molecules and gave the appearance of being smooth. The sample's functional groups can be examined structurally and compositionally using Fourier transform infrared spectroscopy (FTIR) spectroscopy. FTIR spectra were used to examine the functional groups found in the *Psidium guajava* adsorbents in the 399–3999 cm^{-1} wave number range. The FTIR spectra of pretreated *Psidium guajava* loaded with Methylene blue and Methylene blue loading on *Psidium guajava* adsorbent are displayed in Images 30 and 31.

Table 6: FTIR Spectra of Methylene blue onto *Psidium guajava*.

Frequency Cm^{-1}		Assign	Functional Groups
3332	3334	OH-Stretching / Carboxyl	Alcohols/Phenols
1607	1599	C=N,C=C,C=O Stretching	Aldehydes,Ketones,Alkenes
1325	1330	N-O Stretching	Nitro Compounds
1026	1023	C-N	Aliphatic Amines

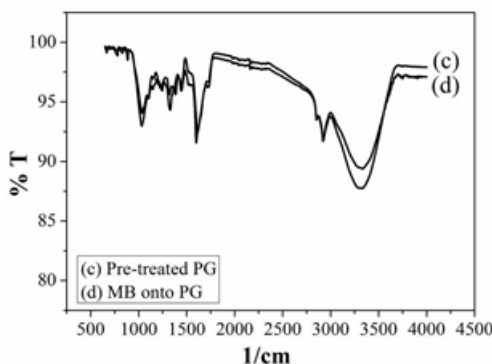


Fig. 32: Images show the FTIR Spectra of *Psidium guajava* adsorbents before and after adsorption of Methylene blue onto its surface.

References

1. A.M. K. Aljebori and A. N. Alshirifi, "Effect of different parameters on the adsorption of textile dye maxilon blue GRL from aqueous solution by using white marble," Asian journal of chemistry, vol. **24**, pp. 5813,(2012).
2. Y. S. Al-Degs, M. I. El-Barghouthi, A. H. El-Sheikh, and G. M. Walker," Effect of solution pH, ionic strength, and temperature on adsorption behaviour of reactive dyes on activated carbon," Dyes and pigments, vol. **77**, pp. 16-23,(2008).
3. V. Gupta, "Application of low-cost adsorbents for dye removal–A review," Journal of environmental management, vol. **90**, pp. 2313-2342, (2009).
4. M. A. M. Salleh, D. K. Mahmoud, W. A. W. A. Karim, and A. Idris, "Cationic and anionic dye adsorption by agricultural solid wastes: a comprehensive review," Desalination, vol. **280**, pp. 1-13, (2011).
5. E. Eren and B. Afsin, "Investigation of a basic dye adsorption from aqueous solution onto raw and pre-treated sepiolite surfaces," Dyes and pigments, vol.**73**, pp. 162-167, (2007).

6. S. Allen and B. Koumanova, "Decolourisation of water/wastewater using adsorption," *Journal of the University of Chemical Technology and Metallurgy*, vol. **40**, pp. 175-192, (2005).
7. S Barbalho, F. Farinazzi-Machado, G. de Alvares, A. S. Brun-nati, and A.
8. Otoboni, "Psidium guajava (Guava): A plant of multipurpose medicinal applications," *Med Aromat Plants*, vol. 1, pp. 2167-0412.1000104, 2012.
9. Z. Aksu, "Application of adsorption for the removal of organic pollutants: a review," *Process biochemistry*, vol. **40**, pp. 997-1026, (2005).
10. G. Crini, "Non-conventional low-cost adsorbents for dye removal: a review," *Bioresource Technology*, vol. **97**, pp. 1061-1085, (2006).
11. H. Lachheb, E. Puzenat, A. Houas, M. Ksibi, E. Elaloui, C. Guillard, and J.-M.Herrmann, "Photocatalytic degradation of various types of dyes (Methylene Blue) in water by UV- irradiated titania," *Applied Catalysis B: Environmental*, vol. **39**, pp. 75-90,(2002).
12. X. Chen, F. Zhang, Q. Wang, X. Han, X. Li, J. Liu, H. Lin, and F. Qu, "The synthesis of ZnO/SnO 2 porous nanofibers for dye adsorption and degradation," *Dalton Transactions*, vol. **44**, pp. 3034-3042, (2015).
13. M. Asgher and H. N. Bhatti, "Evaluation of thermodynamics and effect of chemical treatments on sorption potential of Citrus waste biomass for removal of anionic dyes from aqueous solutions," *Ecological Engineering*, vol. **38**, pp. 79-85, (2012).
14. O. S. Bello, O. M. Adelaide, M. A. Hamed, and O. A. M. Popoola, "Kinetic and equilibrium studies of methylene blue removal from aqueous solution by adsorption on treated sawdust," *Macedonian Journal of Chemistry and Chemical Engineering*, vol. **29**, pp. 77-85, (2010).
15. R. P. Kumar, S. Varanasi, and V. Purushothaman, "Investigation of the adsorption mechanisms of Methylene blue onto press mud through kinetic modeling analysis," *Indian Journal of Science and Technology*, vol. **3**, pp. 44-47, (2010).
16. Y.-S. Ho, R. Malarvizhi, and N. Sulochana, "Equilibrium isotherm studies of methylene blue adsorption onto activated carbon prepared from *Delonix regia* pods," *Journal of Environmental Protection Science*, vol. **3**, pp. 111-116,(2009).
17. P. Wang, M. Cao, C. Wang, Y. Ao, J. Hou, and J. Qian, "Kinetics and thermodynamics of adsorption of methylene blue by a magnetic graphene- carbon nanotube composite," *Applied Surface Science*, vol. **290**, pp. 116-124,(2014).
18. M. Soni, A. K. Sharma, J. K. Srivastava, and J. Yadav, "Adsorptive removal of methylene blue dye from an aqueous solution using water hyacinth root powder as a low cost adsorbent," *International Journal of Chemical Sciences and Applications*, vol. **3**, pp. 338-345, (2012).
19. K. Mundhe, A. Gaikwad, R. Torane, N. Deshpande, and R. Kashalkar, "Adsorption of methylene blue from aqueous solution using *Polyalthia longifolia* (Ashoka) seed powder," *J Chem Pharm Res*, vol. **4**, pp. 423-436,(2012).
20. K. Tong, A. Azraa, and M. J. Noordin, "Isotherms and kinetics studies on the removal of methylene blue from aqueous solution by Gambir," *International Journal of Environmental Science and Development*, vol. **3**, p. 232, (2012).
21. L. Zhou, J. Huang, B. He, F. Zhang, and H. Li, "Peach gum for efficient removal of methylene blue and methyl violet dyes from aqueous solution," *Carbohydrate polymers*, vol. **101**, pp. 574-581, (2014).
22. Hassan, A. Abdel-Mohsen, and M. M. Fouda, "Comparative study of calcium alginate, activated carbon, and their composite beads on methyleneblue adsorption," *Carbohydrate polymers*, vol. **102**, pp. 192-198, (2014).

23. VR Poiba, B Sowjanya, P King, M Vangalapati Advances in Materials and Processing Technologies Removal of methylene blue dye by using synthesised *Grevillea robusta* silver nanoparticles and optimisation of experimental parameters by response surface, 1-15,(2023).
24. B Sowjanya, P King, M Vangalapati Skin of *allium sativum* (garlic) mediated green synthesis of zno nanoparticles and it's adsorption performance for congo red dye removal: kinetic, isotherm and thermodynamic studies European Chemical Bulletin **12** (5), 326-332,(2023)
25. VR Myneni, NR Kanidarapu, SK Kandasamy, M Vangalapati Advanced Microscopy: A Strong Analytical Tool in Materials Science Dyes Adsorption by Nanomaterials: Fixed-Bed Column Studies Using Nano Magnesium Oxide-Loaded Activated Carbon, 259-287,(2022).
26. K Chandrika, A Chaudhary, T Mareedu, U Sirisha, M Vangalapati Adsorptive removal of acridine orange dye by green tea/copper-activated carbon nanoparticles (Gt/Cu-AC np) Materials Today: Proceedings **44**, 2283-2289,(2021).
27. VR Myneni, NR Kanidarapu, M Vangalapati Methylene blue adsorption by magnesium oxide nanoparticles immobilized with chitosan (CS-MgONP): response surface methodology, isotherm, kinetics and thermodynamic studies Iranian Journal of Chemistry and Chemical Engineering (IJCCE) **39** (6), 29-42,(2020).
28. P VenkataRao, G SaiTarun, C Govardhani, B Manasa, PJ Joy Adsorption of congo red dye from aqueous solutions using synthesized silver nano particles of *Grevillea robusta*: Kinetic studies Materials Today: Proceedings **26**, 3009-3014,(2023).